Ultra-Low Phase Noise Oscillators with Attosecond Jitter

Andreas Gronefeld
Ingenieurbüro Gronefeld, Germany
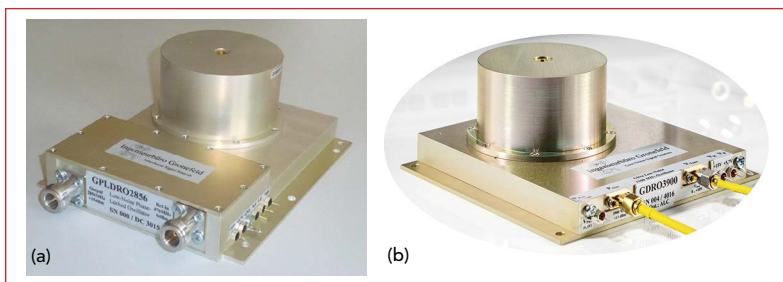
*Two designs of ultra-low noise dielectric-resonator oscillators (DRO) for 2.856 GHz[1] and 3.9 GHz[2] with sub-femtosecond jitter (shown in **Figure 1**) are reviewed. This work was motivated by contracts with research institutions Deutsches Elektronen-Synchrotron,[3] Hamburg, Germany and Pohang Accelerator Laboratories,[4] Pohang, Korea that require this level of performance for optimum operation of their X-ray Free Electron Laser (X-FEL) installations. However, other applications like the microwave synthesizers found in Caesium-Fountain atomic clocks or high performance radars also may benefit from ultra-low noise signal sources of this kind. And the design methodology presented can, in principle, be transferred to any frequency in the 1 to 20 GHz range.*

X-FELs are still a rare breed of research facilities, with just four installations worldwide that are capable of generating extremely intense (GWatts), ultra-short (20 to 50 fs) flashes of coherent radiation, reaching down to and below 0.1 nm wavelength (see *Figure 2*). These short-wavelength ("hard") X-rays are in high demand by researchers for imagery at the molecular, atomic and even subatomic level.[5-6] Even more unique, the ultra-short flashes allow sampling of the dynamics of atomic bonds or chemical reactions to generate video-like sequences of those picosecond processes[7-8] at the atomic level.

X-FELs work by accelerating bunches of electrons to extremely high energies (10 to 20 GeV) and converting a small amount to coherent X-rays of a very narrow spectral range. The "lasing" action takes place in a long chain (> 100 m) of alternating polarity magnets, called "undulators,"[9] and requires the accelerated electrons to have a very small energy spread (see *Figure 3*).

The acceleration process makes use of a microwave signal (mostly 2.856 or 1.3/3.9 GHz), distributed throughout the installation and amplified in many substations to tens of megawatts of pulse power. Each high-power amplifier drives a group of cavity resonators, (forming a long chain of up to 1700 m), with their extremely large electromagnetic fields propelling the electrons forward. For optimum energy transfer, the phase relationship of the microwave signal must be precisely matched to the locus of the electron bunch. Phase stability to 0.01° (10 fs at 3 GHz) is needed for optimum acceleration with minimal energy spread and the ability to compress the electron bunch down to femtosecond duration and maintain it.

The targeted phase stability requires extremely stable signal sources, containing jit-

▲ Fig. 1 2.856 GHz PL-DRO (a) and 3.9 GHz DRO (b).

ter ideally to just a few femtoseconds. But how does this relate to phase noise, the quantity usually used to describe the short term stability of a signal source?

JITTER VERSUS PHASE NOISE

While the phase noise spectral density function $L(f_m)$ completely describes the short term stability of a signal source, phase jitter, the measure of the output waveform zero-crossing's time deviation, is computed by integrating $L(f_m)$ over a certain offset frequency range, implying that jitter numbers must always be accompanied by that integration range and can only be compared when the integration ranges match.

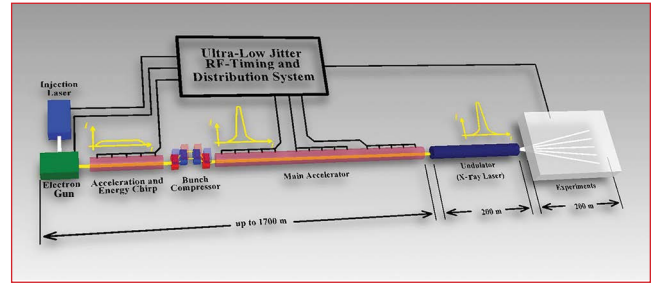$$J = \frac{1}{2\pi f_0}\sqrt{2\int_{f_1}^{f_2} L(f_m)df} \qquad (1)$$

Computing jitter with Equation 1 neglects all contributions of the phase noise spectrum below f_1 and above f_2 and is well justified, if f_1 and f_2 are chosen in a meaningful way for a given system. Typically a system has a "maximum observation time," defining f_1 (slower phase changes do not alter the system's output) and a "maximum processing bandwidth," that sets f_2 (faster phase changes are not processed by the system).

In FELs, the processing bandwidth ranges from 10 to 30 MHz, with 100 MHz on the horizon, giving a first hint at what to look for in designing a low jitter signal source, as the higher f_2, the more important a low oscillator noise floor becomes.

With the lower bound f_1 typically specified as 1 Hz, to ensure pulse to pulse stability and keep low frequency noise from interfering with drift countering measures, signal sources for FELs are always a combination of a microwave oscillator that defines phase noise from 1 to 10 kHz to f_2, phase locked to quartz crystal oscillators, determining phase noise from 1 Hz to 1 to 10 kHz. For the oscillators discussed here, jitter numbers integrating phase noise over 1 kHz to 30 MHz or 10 kHz to 30 MHz are relevant.

ULTRA-LOW PHASE NOISE OSCILLATOR DESIGN

There are only a few elements needed to build an oscillator: a (lossy) resonator to set the frequency, an amplifier to compensate the resonator's losses and both arranged in a feed back loop.
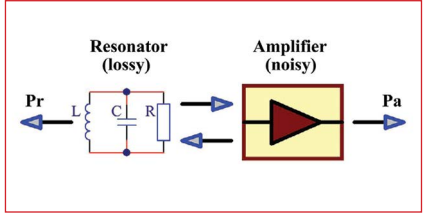

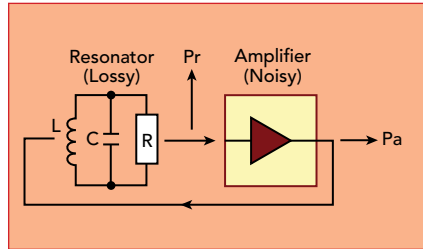▲ Fig. 3 Simplified X-FEL block diagram.

Oscillator Topologies

The first decision in designing an oscillator involves how the amplifier and resonator are coupled in a feedback arrangement. Most oscillators use the "reflection" type topology shown in *Figure 4* (negative resistance oscillator[10]). Note the possibility of either taking the oscillator's output power (Po) from the amplifier (Pa) or coupling to the resonator (Pr). This topology, albeit simple, has the drawback that a number of important parameters like resonator loading, output power and amplifier compression are tightly coupled and hard to control separately.

▲ Fig. 4 Reflection oscillator topology.

▲ Fig. 5 Transmission oscillator topology.

For narrowband sources, the topology of a transmission type oscillator, shown in *Figure 5*, gives much better control of the critical parameters, is widely used[11-13] and chosen here. Again, the designer has the choice to take the output power from the amplifier (Pa), maximizing Po, or from the resonator (Pr). The latter reuses this element as a filter to suppress the amplifier's broadband noise outside the resonator's passband,[12,14] outweighing the loss of signal power that is easily compensated by a following buffer amplifier. Using this topology (see *Figure 6*) is key to achieving low noise floors of -180 dBc/Hz (see trace 6 in *Figure 7*).
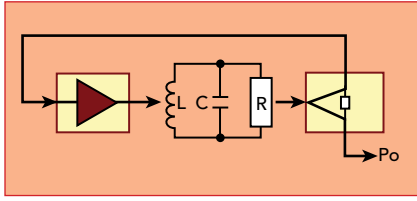
Oscillator Optimization for Low Noise

For determining what measures need to be taken to arrive at a low noise, low jitter oscillator, the old phase noise model of Leeson[15] is still helpful:

$$L(f_m) = 10\log\left[\frac{1}{2}\frac{FkT}{P_s}\left(\left(\frac{f_0}{2Q_L f_m}\right)^2 + 1\right)\left(\frac{f_c}{f_m} + 1\right)\right] \qquad (2)$$

It relates the single sideband (SSB) phase noise L (in dBc/Hz) as a function of the offset frequency f_m around

Fig. 6 Optimum transmission oscillator topology.

centre frequency f_0 to four important parameters. To minimize noise, this model dictates:
- Maximize S/N in the loop, by maximizing signal power P_S with respect to noise power FkT (F: noise factor).
- Maximize the loaded Q. $Q_L = f_0/BW_{3dB}$ of the resonator.
- Minimize the amplifier's flicker corner frequency f_c.

Figure 7 shows a number of simulated phase noise diagrams and the influence of those four parameters. Obviously, optimizing Q_L is of most efficiency, as it enters Equation 2 squared. Less obvious, the highly device technology dependent f_c can have a huge impact, as it is not unusual to find GaAs devices to have 100x higher 1/f-noise corner frequencies than their silicon counterparts.

Resonator Q, Unloaded/Loaded

For single-frequency oscillators, dielectric resonators placed inside a metallic cavity offer the highest Q and for the frequencies discussed here, resonators with unloaded Q (Q_U) of 30,000 at 2.856 GHz and 25,000 at 3.9 GHz were obtained.

Coupling to the resonator (loading it) reduces Q_U to Q_L and Parker[16] established that optimum coupling should occur at S_{21} = -6 dB, where Q_L = 1/2 Q_U. This coupling factor, leading to Q_L of 15,000, was used for the 2.856 GHz design. For 3.9 GHz, the reasoning[16] was questioned, as 2 dB better phase noise can be achieved by looser coupling with a resonator insertion loss of 9 dB. The necessary increase in amplification and output power by 3 dB also increases the amplifiers output noise power by 3 dB, but that increase gets suppressed by the resonator's filtering action. With the above choice, the 3.9 GHz-design was also realized with a Q_L of 15,000, despite the lower Q_U.

Amplifier Optimization

The most crucial design decision in the amplifier electronics involves selection of the active device. Here,

bipolar silicon transistors are preferred to ensure low f_c. Also, designing for high output power pays off, as it lowers the noise floor. Finally, as with all oscillator designs, the device's transition frequency should be as low as practically possible for building an amplifier with acceptable gain.

That gain has to be some dB above the losses in the loop to accommodate variations over temperature and account for the resonator's amplitude response over the tuning range. Of course, the occurring gain compression must not lead to instabilities of the amplifier. Low noise device biasing was added to the amplifier design in a two tier regulation scheme that virtually eliminates frequency pushing.
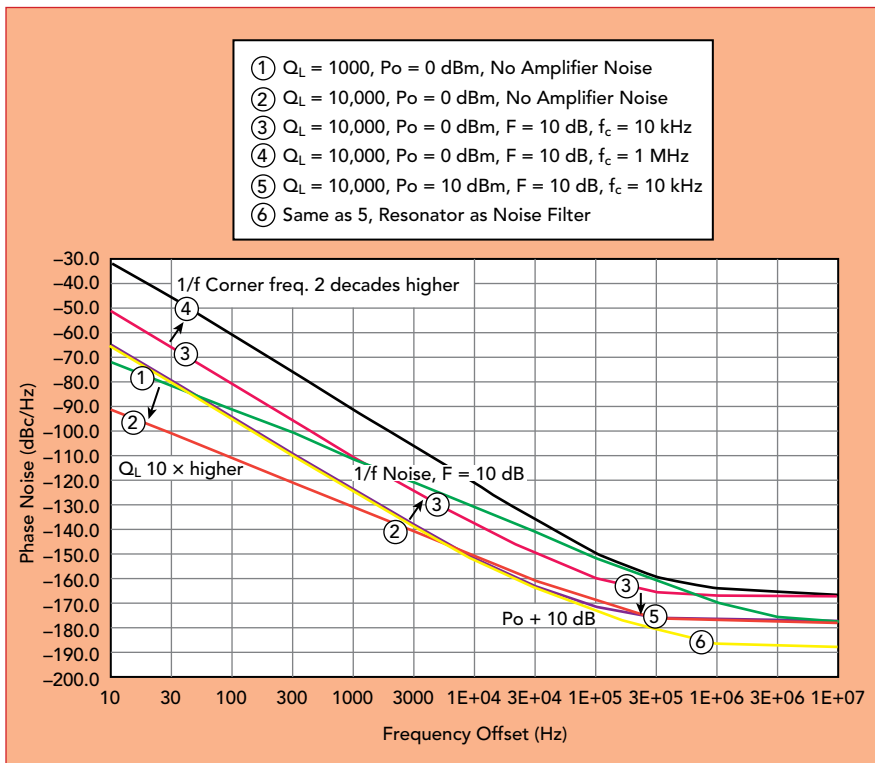
Add-Ons

No oscillator is complete without a buffer amplifier that isolates the oscillator sufficiently from the load. For both designs, double stage buffers were built, reducing pulling to < 1 ppm with a fully reflecting load over all angles, while keeping the noise floor at -180 dBc/Hz. Also an ALC was added to stabilize output power to < 0.1 dB, helping reduce phase drifts, due to (tuning induced) amplitude changes.
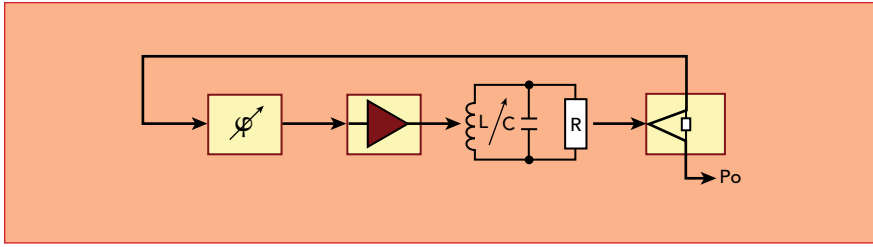
Temperature Stability

Frequency tuning of a DRO can be done by either tuning the resonator or varying the phase in the loop (see *Figure 8*). Most high performance DROs[10-13] and the designs presented here provide a coarse mechanical tuning of the resonator (some MHz) and use a phase-shifter (PS) for electronic tuning. Electronic tuning of the resonator, though possible,[17] risks degradation of Q as it involves coupling to varactor diodes that have much higher losses.
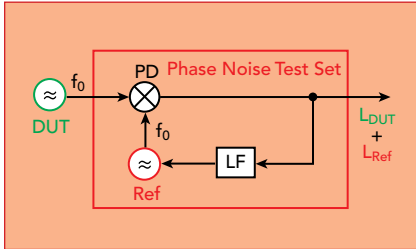
The available frequency shift from an in-loop PS, however, is confined to a portion of the resonator bandwidth (-2 dB points in this case). With a Q_L of 15,000, the tuning range amounts to ±25 ppm. This poses a problem, when the temperature coefficient (TC) of the resonator assembly becomes too high with respect to the targeted temperature range. On top, metallic enclosure (cavity) and dielectric resonator (puck) have different TCs

① Q_L = 1000, Po = 0 dBm, No Amplifier Noise
② Q_L = 10,000, Po = 0 dBm, No Amplifier Noise
③ Q_L = 10,000, Po = 0 dBm, F = 10 dB, f_c = 10 kHz
④ Q_L = 10,000, Po = 0 dBm, F = 10 dB, f_c = 1 MHz
⑤ Q_L = 10,000, Po = 10 dBm, F = 10 dB, f_c = 10 kHz
⑥ Same as 5, Resonator as Noise Filter

Fig. 7 Oscillator phase noise from Equation 2 with varying parameters.

▲ Fig. 8 **Frequency tuning the transmission oscillator.**

▲ Fig. 9 **Typical phase noise test setup.**

▲ Fig. 10 **Phase noise measurement of 3.9 GHz DRO with noisy reference.**

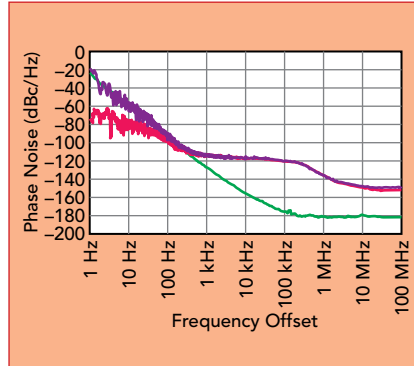with, even worse, different time responses.[12,18]

With the aluminium cavity at -1 ppm/K and the 2.856 GHz resonators at +1.5 ppm/K, both TCs cancel well enough, such that this DRO design has no problem to safely operate over a 0°C to 50°C temperature range, more than adequate for the highly temperature controlled accelerator environments.

The -3 ppm/K TC of the 3.9 GHz resonators, however, adds to the cavity's TC and allows for just ±6°C of temperature variation that can be compensated with the electronic tuning. As this was felt to be insufficient, a mild sort of oven was incorporated, keeping the assembly at +35°C for long time reliable operation.

As the problem of temperature drift mounts with rising Q_L, it will be even more pronounced at lower frequencies (e.g. 1.3 GHz), where Q_L may increase to 30,000 or more, leaving ±12 ppm or less to be electronically compensated. Meeting this challenge either requires further oven control and thermal insulation or alternative means of electronically tuning the resonator.

Phase Noise Measurement Techniques and Challenges

Measurement of phase noise is a time measurement and as such carried out by comparing two clocks. In addition to the oscillator, or device, under test (DUT), a second oscillator (reference clock) of the same

frequency is needed and the time (phase) difference between both oscillators is recorded using a phase detector (PD) (see **Figure 9**).

However, the PD's output is a measure of the sum of the DUT's and the reference's noise power. As long as the reference clock is known to have, say, > 10 dB lower noise than the DUT, the measurement yields a correct result within ±1 dB.

Commercial phase noise test sets[19-23] that cover wide frequency ranges, however, incorporate microwave synthesizers as reference clocks. With the phase noise of those synthesizers being decades higher than the phase noise of the oscillators presented here, simple phase detection will not produce the phase noise of the DUT, but rather that of the measurement device's synthesizer. **Figure 10** shows such a measurement (purple trace) that for f_m > 300 Hz reproduces the noise of the reference (red trace), whereas the true result of the 3.9 GHz DRO is actually the green trace.

Phase Noise Measurement Using Cross Correlation

A clever way out of this dilemma, enabling phase noise test sets to measure sources with far less noise than their reference has, is the use

of a second identical test set, with a second independent reference clock. By letting both test sets measure the DUT simultaneously and combining their outputs by a cross-correlator, it is possible to bring down the noise of the test sets considerably (see **Figure 11**).

In fact, this cross-correlation technique, that most commercially available phase noise test sets today offer, theoretically, leads to a noise-free test set. The scheme works by transforming the output of the two PDs into the spectral domain (FFT), multiplying them and storing the result. The process is repeated (theoretically forever!) and all stored results are averaged. Mathematically this is represented by:

$$\overline{\left(S_{DUT} + S_{R1}\right)\left(S_{DUT} + S_{R2}\right)} = \overline{\left(S_{DUT}\right)^2} + \overline{S_{DUT}S_{R1}} + \overline{S_{DUT}S_{R2}} + \overline{S_{R1}S_{R2}} \quad (3)$$

It is important to note that the first term of the right hand side is the phase noise spectral density of the DUT, L_{DUT}. The remaining three terms on the right hand side are called cross-spectral densities, relating two different noise processes and whenever two noise processes are uncorrelated, these quantities are known to be zero.

$$\overline{\left(S_{DUT} + S_{R1}\right)\left(S_{DUT} + S_{R2}\right)} = L_{DUT} \quad (4)$$

So in order to build a noise-free phase noise test set, the noise sources n_{R1} and n_{R2} in the two test sets must be uncorrelated and the measurement must be carried out forever (ideal averaging requires infinite summations). While the first requirement can be sufficiently fulfilled by sound engineering, the latter requirement is disillusioning, as it ruins the perspective of a noise-free test set in practice.

Yet, the technique is very powerful, as it reduces the test set noise by:

$$5\log_{10}(N) \quad [dB] \quad (5)$$

with N the number of cross spectra averaged. So for every 10-fold lengthening of measurement time, 5 dB noise reduction is gained.
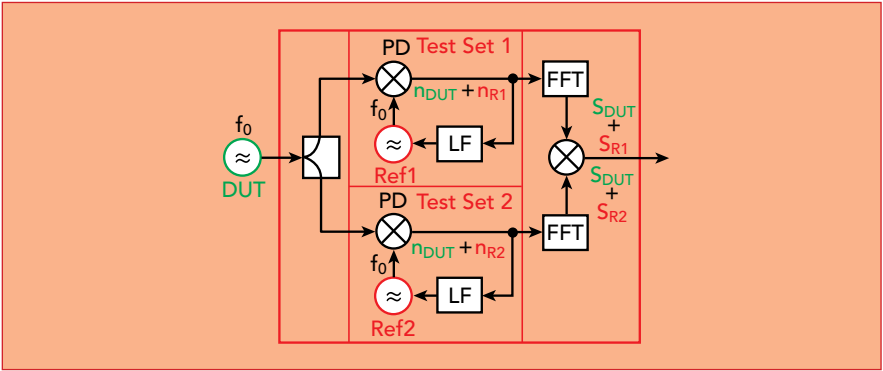
It must be stressed that measurement sensitivity with the cross-

correlation technique is solely dependent upon measurement time. Most commercial instruments[19-23] allow the user to input the number of 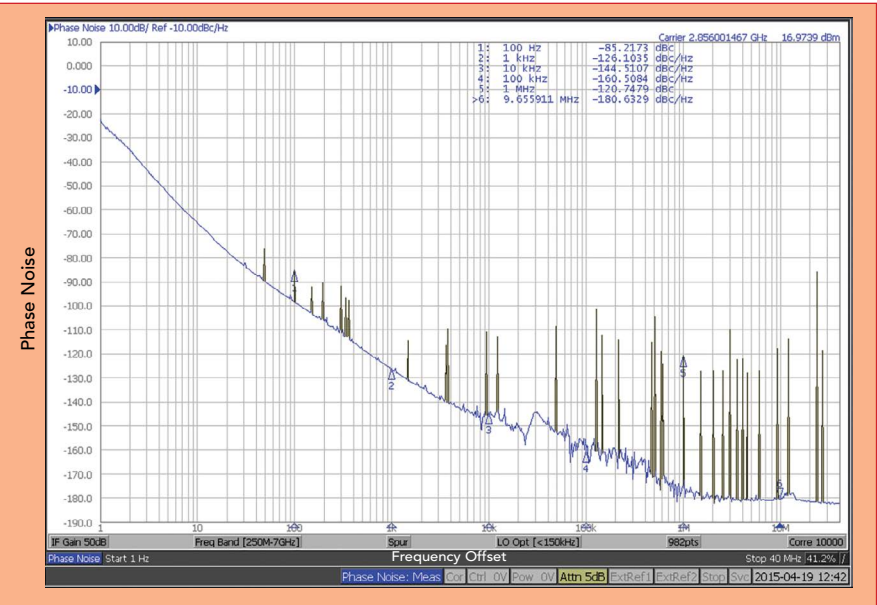cross spectra to be averaged as the lever to set sensitivity and measurement time. Less obvious, lowering the start frequency by a decade also lengthens measurement time by a factor of 10 and yields a 5 dB gain in sensitivity. This is because in the time it takes to collect sufficient samples for one correlation in the lowest offset frequency decade (e.g. 1 to 10 Hz), 10x the amount of data is available in the adjacent decade (10 to 100 Hz), allowing 10 cross spectra to be computed and averaged here.
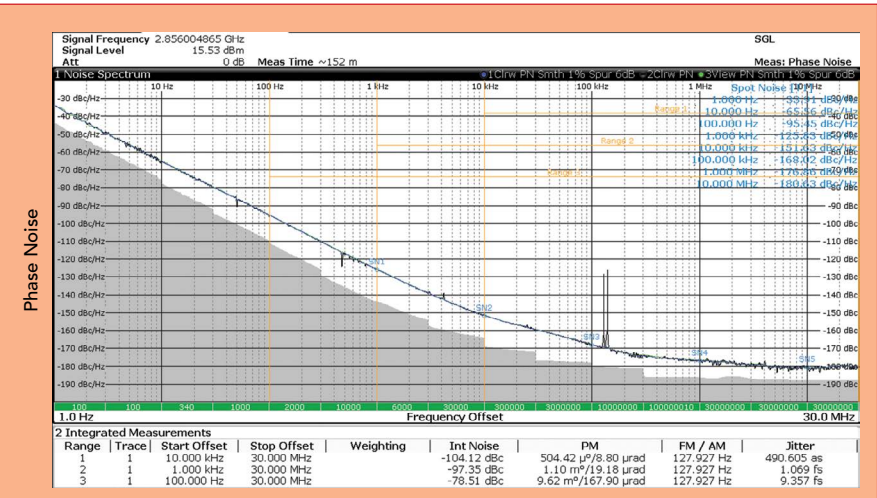
This pattern continues up to the stop frequency of the measurement. Lowering the start frequency by one decade usually has the same effect as increasing the correlations setting by a factor of 10, simply because both steps lead to an increase in measurement time by a factor of 10.

▲ **Fig. 11** Cross-correlation test setup.

▲ **Fig. 12** Measurement of the 2.856 GHz DRO using a test setup with maximum sensitivity (36 h).
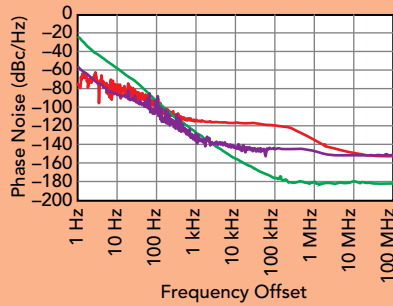

▲ **Fig. 13** Measurement of the 2.856 GHz DRO using R&S test setup with about 2.5 h measurement time.
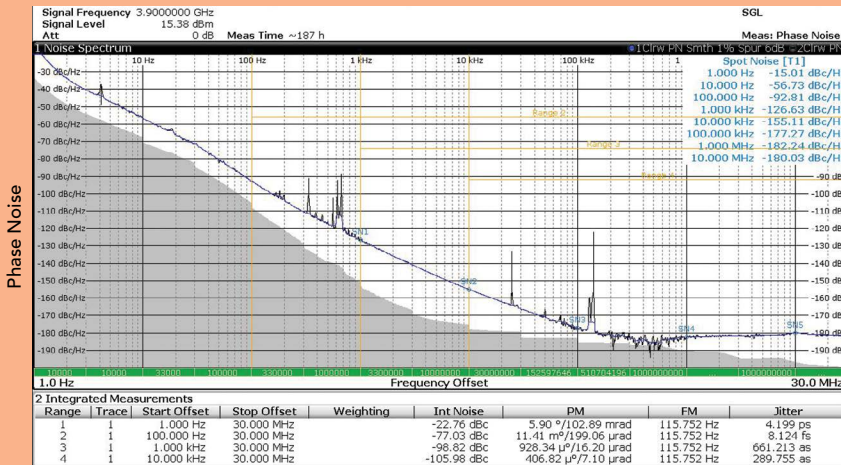
Measurement Results

With the development of the 2.856 GHz DRO, it soon became apparent that the sensitivity of the then used phase noise test set[21] was insufficient. *Figure 12* shows a measurement, taken with the maximum number of correlations (and minimum offset start frequency), extending over 36 hours. Yet, the plot still shows insufficient sensitivity between 10 kHz and 1 MHz, as well as artefacts around 30 kHz.

Also development work on the DROs was tedious, as phase noise measurements took at least 20 minutes in order to come up with a useable value at 1 kHz offset. Since the DRO's -125 dBc/Hz at that offset are just 10 dB below the test set's synthesizer noise, a manageable number of correlations yields an acceptable result (compare to Figure 10).

The situation much improved with the availability of a phase noise measurement system with much lower noise internal reference sources. *Figure 13* shows a measurement of the 2.856 GHz DRO with this instrument taken over about 2.5 h of measurement time, showing excellent accuracy. *Figure 14* shows 20 dB less phase noise (purple trace) over the offset frequency range from 1 kHz to 100 kHz, compared to another instrument (red trace). Recalling that the cross correlation technique reduces test set noise by 5 dB for every 10-fold lengthening of measurement time, the 20 dB reduction in synthesizer phase noise translates to a potential gain in measurement speed of four decades.

Fig. 14 Comparison of various test setup phase noise compared to 3.9 GHz DRO.

Fig. 15 Measurement results for the 3.9 GHz DRO.

Going back to Figure 13, the alert designer will notice that the phase noise of this DRO does not decay with 20 dB to 30 dB/decade into the noise floor, as theory demands. The measurement therefore hints at extra noise polluting the signal for offsets above 10 kHz, suggesting potential for improvement, not evident from Figure 12. Further investigations revealed a number of simple to implement changes that were incorporated into the next design of the 3.9 GHz DRO. Additional performance was gained by tweaking the design through phase noise optimizations, enabled by the measurement speed of the system that makes useable phase noise data at 1 kHz/10 kHz offset available in less than 10 seconds, even at those challenging phase noise levels. The measurement results of the 3.9 GHz DRO are shown in *Figure 15*.

With both designs built around dielectric resonators with a loaded Q of 15,000, phase noise numbers at 3.9 GHz can be expected to be 2.7 dB = $20\log_{10}(3.9/2.856)$ higher than at 2.856 GHz. Instead, for offsets over 1 kHz, the 3.9 GHz design shows even lower phase noise. In terms of jitter, the optimizations yielded a 40 percent reduction, bringing jitter down to 0.66 fs (integrating phase noise over 1 kHz to 30 MHz) and 0.29 fs (10 kHz to 30 MHz).

CONCLUSION

Sub-femtosecond jitter microwave sources were developed for two of the relevant frequencies in X-FEL electron beam accelerators. None of the critical design decisions taken are novel, but rather adhere to long known principles. Use of modern, low noise components and techniques, as well as careful optimization of all building blocks was key to the achieved performance.

It should be pointed out that the

resulting designs are stable and reproducible commercial products, with typical noise data not differing by more than a few dB. With the phase noise of the realized oscillators being, at most offsets, decades below the intrinsic noise of most measurement systems, such low noise sources can only be measured using cross-correlation techniques. Yet, the required sources to compare the DRO against must be as low noise as possible, to not overburden the cross-correlation capabilities, bearing in mind that every 5 dB of necessary test set noise reduction require a 10-fold measurement time.■

References

1. GDRO2856 Datasheet, Ingenieur-büro Gronefeld, www.gronefeld.de.
2. GDRO3900 Datasheet, Ingenieur-büro Gronefeld, www.gronefeld.de.
3. DESY Homepage, www.desy.de/index_eng.html.
4. Pohang Accelerator Laboratory (PAL), http://pal.postech.ac.kr/paleng.
5. "FLASH Looks Deep into the Atom," *DESY-News*, www.desy.de/news/news_search/index_eng.html?openDirectAnchor=758.
6. "First Atomic Structure of an Intact Virus Deciphered with an X-ray Laser," *DESY-News*, www.desy.de/news/news_search/index_eng.html?openDirectAnchor=1240.
7. "New 'Molecular Movie' Reveals Ultrafast Chemistry in Motion," *SLAC-News*, www6.slac.stanford.edu/news/2015-06-22-new-%E2%80%98molecular-movie%E2%80%99-reveals-ultrafast-chemistry-motion.aspx.

8. "High Speed Camera Snaps Bio-Switch in Action," *DESY-News*, www.desy.de/news/news_search/index_eng.html?openDirectAnchor=1138.

9. "Undulator," *Wikipedia*, https://en.wikipedia.org/wiki/Undulator.

10. J. Piekarski and K. Czuba, "The Method of Designing Ultra-Low Phase Noise DROs," *MIKON 2010*.

11. W. J. Tanski, "Development of a Low Noise L-Band Dielectric Resonator Oscillator," *IFCS 1994*.

12. P. Stockwell, D. Green, C. McNeilage and J.H. Searls, "A Low Phase Noise 1.3 GHz DRO," *IFCS 2006*.

13. J. Everard and K. Theodoropoulus, "Ultra-Low Phase Noise Ceramic based DROs," *IFCS 2006*.

14. M. M. Driscoll, "Low Noise, VHF Crystal Oscillator Utilizing Dual, SC-Cut Resonators," *UFFC 1986*.

15. D.B. Leeson, "A Simple Model of Feedback Oscillator Noise Spectrum," *Proc. of IEEE*, Vol. 54, 1966.

16. T. E. Parker, "Current Developments in SAW Oscillator Stability," *ASFC 1977*.

17. A. Effendy and W. Ismail, "Wide Tuning Range Dielectric Resonator by Optimizing the Tuning Stub Characteristic Impedance," *APMC 2012*.

18. M. J. Loboda, T. E. Parker and G. K. Montress, "Temperature Sensitivity of Dielectric Resonators and Dielectric Resonato Oscillators," *AFCS 1988*.

19. Phase Noise Analyzer APPH20G, AnaPico Ltd.

20. Phase Noise Analyzer HA7062B/C, Holzworth Instrumentation Inc.

21. Signal Source Analyzer E5052B, Keysight Technologies Inc.

22. Phase Noise Analyzer NXA, Noise eXtended Technologies S.A.S.

23. Phase Noise Analyzer FSWP, Rohde & Schwarz GmbH & Co. KG.